A Functionalized Noncovalent Macrocyclic Multiporphyrin Assembly from a Dizinc(II) Bis-Porphyrin Receptor and a Free-Base Dipyridylporphyrin

Elisabetta Iengo,*[a, b] Ennio Zangrando,[a] Enzo Alessio,[a] Jean-Claude Chambron,[b, c] Valérie Heitz,[b] Lucia Flamigni,*[d] and Jean-Pierre Sauvage*[b]

Abstract: The bis-porphyrin system $\mathbf{ZnP_2}$, in which two zinc porphyrins are connected by a phenanthroline linker in an oblique fashion, acts as a bifunctional receptor towards the complexation of free-base *meso*-5,10-bis(4′-pyridyl)-15,20-diphenylporphyrin (**4′-*cis*DPyP**). In solution, NMR spectroscopy evidenced quantitative formation of the tris-porphyrin macrocyclic assembly $\mathbf{ZnP_2}$**(4′-*cis*DPyP)**, in which the two fragments are held together by two axial 4′-N(pyridyl)–Zn interactions. The remarkable stability of the edifice (an association constant of about $6 \times 10^8\,\mathrm{M}^{-1}$ was determined by UV/Vis absorption and emission titration experiments in toluene) is due to the almost perfect geometrical match between the two interacting units. The macrocycle was crystallized and studied by X-ray diffraction, which confirmed the excellent complementarity of the two components. Photoinduced energy transfer from the singlet excited state of the zinc porphyrin chromophores to the free-base porphyrin occurs with an efficiency of 98% ($k_{en} = 2 \times 10^{10}\,\mathrm{s}^{-1}$ in toluene, ambient temperature) with a mechanism consistent with a dipole–dipole process with a low orientation factor.

Keywords: antenna systems · energy transfer · macrocycles · porphyrinoids · self-assembly

Introduction

The elaboration of noncovalent multiporphyrin assemblies is an important challenge with regard to mimicking the bacterial photosynthetic reaction center (RC),[1] light-harvesting antenna complexes (LH1 and LH2),[2] and electron transfer processes in proteins containing several heme groups.[3] Convenient synthetic strategies exploit the formation of coordinative bonds, multiple hydrogen bonds, or both.[4] A few recent examples leading to elaborate cyclic structures are particularly noteworthy.[5]

Oblique dizinc(II) bis-porphyrin systems **I**, consisting of an organic spacer that connects two zinc porphyrin moieties in a V-shaped and roughly cofacial disposition, have been employed for the construction of stable, noncovalently linked assemblies by means of multiple ligand–metal interactions or multiple hydrogen bonds. The length and the flexibility of the

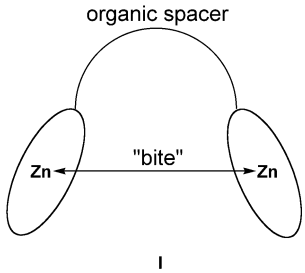

I

organic spacer usually define the interporphyrin separation of the host cavity (bite), a crucial parameter in determining the affinity for guests of different sizes. Complexation of an easily reducible ditopic guest such as dipyridylbenzoquinone,[6a] pyromellitimide[6b, c] or naphthalene imide[6c, d] by means of two simultaneous zinc–nitrogen interactions allowed the

[a] Dr. E. Iengo, Prof. E. Zangrando, Prof. E. Alessio
Dipartimento di Scienze Chimiche, Università di Trieste
Via L. Giorgieri 1, 34127 Trieste (Italy)
Fax: (+39) 40-5583903
E-mail: iengo@dsch.univ.trieste.it

[b] Dr. E. Iengo, Dr. J.-C. Chambron, Dr. V. Heitz, Dr. J.-P. Sauvage
Laboratoire de Chimie Organo-Minérale, UMR 7513 du CNRS
Université Louis Pasteur, Faculté de Chimie
4, rue Blaise Pascal, 67070 Strasbourg Cedex (France)

[c] Current address:
Dr. J.-C. Chambron
LIMSAG, UMR 5633 du CNRS
Université de Bourgogne, Faculté des Sciences "Gabriel"
6, boulevard Gabriel, 21000 Dijon (France)

[d] Dr. L. Flamigni
Istituto ISOF-CNR
Via P. Gobetti 101, 40129 Bologna(Italy)
Fax: (+39) 51-639-9844
E-mail: flamigni@isof.cnr.it

Supporting information for this article is available on the WWW under http://www.chemeurj.org/ or from the author. Tables of crystal data, VT ^{1}H NMR spectra ($CDCl_3$) of H2,6 and H3,5 resonances of $\mathbf{ZnP_2}$**(4′-*cis*DPyP)** (**1**), low-*T* H,H-COSY spectrum of **1**, absorption spectra of $\mathbf{ZnP_2}$, **4′-*cis*DPyP**, and **1**.

 DOI: 10.1002/chem.200304795

assembly of donor–acceptor systems capable of undergoing photoinduced electron transfer processes from the porphyrin host to the encapsulated guest. In addition, porphyrins bearing peripheral heteroatoms for coordination to Zn have been also used as guest molecules, and they allow the study of interporphyrin photoinduced energy-transfer processes.[7, 8] None of these multiporphyrin assemblies was structurally characterized in the solid state.

Similar oblique bis-porphyrin systems were investigated for their molecular recognition capabilities, such as enantiomeric discrimination of amino acids,[9a–c] amines,[9d] and sugars,[9e] and for the formation of three-dimensional capsules.[9f–h]

Some of us have worked extensively on the synthesis of rotaxanes incorporating porphyrins.[10] In early work, the isolated dumbbell of the rotaxanes, consisting of an oblique dizinc(II) bis-porphyrin with a 1,10-phenanthroline spacer (**ZnP_2**, Scheme 1), was prepared separately and used in energy- and electron-transfer studies.[11]

The X-ray structure of **ZnP_2** showed that the center-to-center distance between the zinc porphyrin rings (Zn···Zn) is about 13.5 Å.[12] When these structural data were applied to CPK models, they suggested that good complementarity could be achieved with 5,10-bis(4′-pyridyl)-15,20-diphenylporphyrin (**4′-*cis*DPyP**), a *meso*-4′-*cis*-dipyridylporphyrin with an N···N distance of about 10.7 Å, under the assumption of an average axial Zn–N bond length of 2.2 Å. Thus, we expected that treatment of **ZnP_2** with **4′-*cis*DPyP** should lead to formation of a stable 1:1 macrocyclic adduct.

We demonstrate here that formation of the expected macrocyclic assembly **ZnP_2(4′-*cis*DPyP)** (36-membered ring) is quantitative in solution, as evidenced by ^{1}H NMR spectroscopy and UV/Vis absorption and emission titration experiments. Its structure could be further detailed by X-ray crystallography. The new assembly shows photoinduced intramolecular energy transfer, the parameters of which are in agreement with a Förster mechanism characterized by unfavorable interactions of transition dipole moments.

Results and Discussion

NMR spectroscopy: ^{1}H NMR spectroscopy established that addition of stoichiometric amounts of **4′-*cis*DPyP** to a solution of **ZnP_2** in $CDCl_3$ leads readily to quantitative formation of **ZnP_2(4′-*cis*DPyP)** (**1**), a 1:1 macrocyclic adduct in which **4′-*cis*DPyP** is encapsulated between the two oblique zinc porphyrin units of **ZnP_2** by axial ligation of the pyridyl N atoms to the Zn atoms (Scheme 1).

Titration of **ZnP_2** with **4′-*cis*DPyP** in $CDCl_3$ results in the appearance of sharp signals for coordinated **4′-*cis*DPyP** in the 1:1 complex **1**, the intensity of which increases till the stoichiometric ratio between the reagents is reached. No signal for uncoordinated **4′-*cis*DPyP** was observed. The signals of **ZnP_2** are only slightly affected by progressive addition of **4′-*cis*DPyP**, and this indicates that the symmetry of **ZnP_2** is maintained in the adduct (see below). When the stoichiometric ratio is reached, the H2,6 and, to a minor extent, the H3,5 resonances of the **4′-*cis*DPyP** pyridyl rings bound to zinc broaden, but they sharpen again on lowering the temperature to below 0 °C.[13] This broadening indicates that when formation of the 1:1 adduct from the reagents is complete, **4′-*cis*DPyP** in **1** is involved in a relatively fast dissociation equilibrium, which becomes apparent in the absence of excess **ZnP_2**.

Below 0 °C the resonances of the **4′-*cis*DPyP** pyrrole protons (β-H) and of the internal NH protons, together with some of the resonances of **ZnP_2**, first broaden and eventually split below −40 °C, that is, dynamic processes are present in **1** (Figure 1). Since the downfield region of the ^{1}H NMR spectrum of **1** is quite crowded, a combination of 2D H,H-COSY and NOESY-EXSY experiments at different temperatures was needed for complete assignment of the signals of **1**.

We examine first the main features of the ambient-temperature ^{1}H NMR spectrum of **1** that unambiguously establish the nature and geometry of the adduct: 1) Relative integration of **4′-*cis*DPyP** and **ZnP_2** signals indicates that a 1:1 adduct is quantitatively formed. 2) Axial coordination of **4′-*cis*DPyP** is unequivocally established by the overall upfield shifts of its resonances due to the combined effects of the ring currents of the two zinc porphyrin units of **ZnP_2**. This effect is particularly large for the pyridyl H2,6 and H3,5 protons ($\Delta\delta$ = −6.06 and −1.90, respectively).[13, 14] The pyridyl protons of **4′-*cis*DPyP** give rise to only two equally intense signals, which implies that the two pyridyl rings are equivalent and symmetrically coordinated. 3) The pattern of the pyrrole protons (βH) of **4′-*cis*DPyP**, two singlets and two doublets of equal

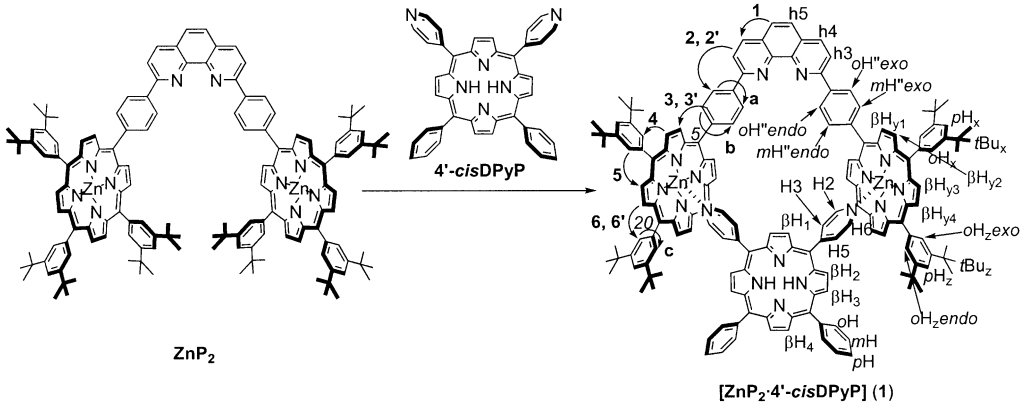

Scheme 1. Schematic synthesis of **1** with labeling scheme. NOE and exchange connections observed in the 2D NOESY-EXSY spectrum at −40 °C are indicated by numbers and letters, respectively. The numbering scheme for NOE connections and labels for exchange connections refer to Figure 2.

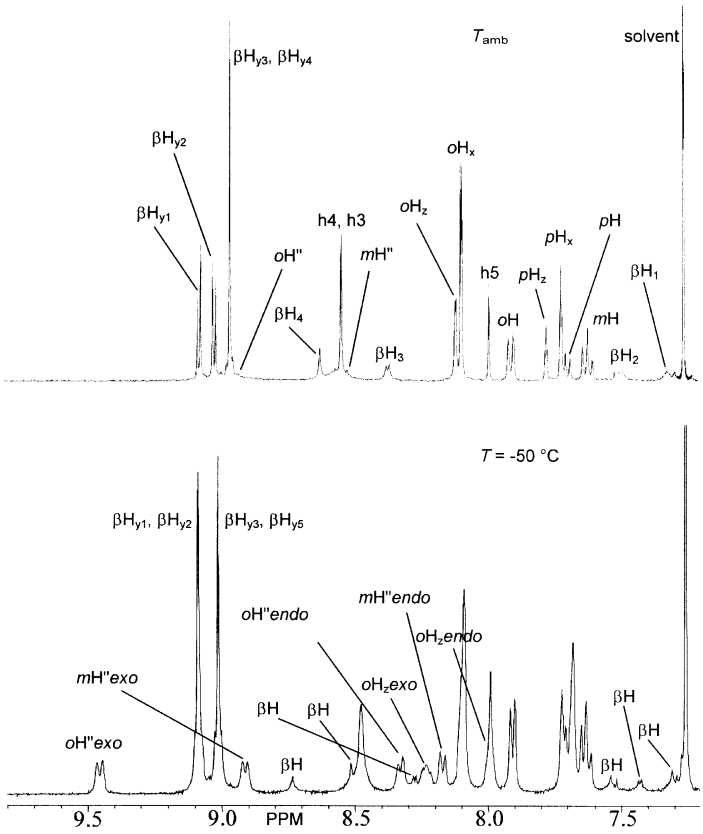

Figure 1. ^{1}H NMR spectrum ($CDCl_3$) of **1** at ambient temperature (top) and at $-50\,^{\circ}C$ (bottom); upfield region with H3,5, H2,6, tBu$_x$, tBu$_y$, and NH resonances is omitted. See Scheme 1 for labeling scheme and Supporting Information for H,H-COSY cross-peaks.

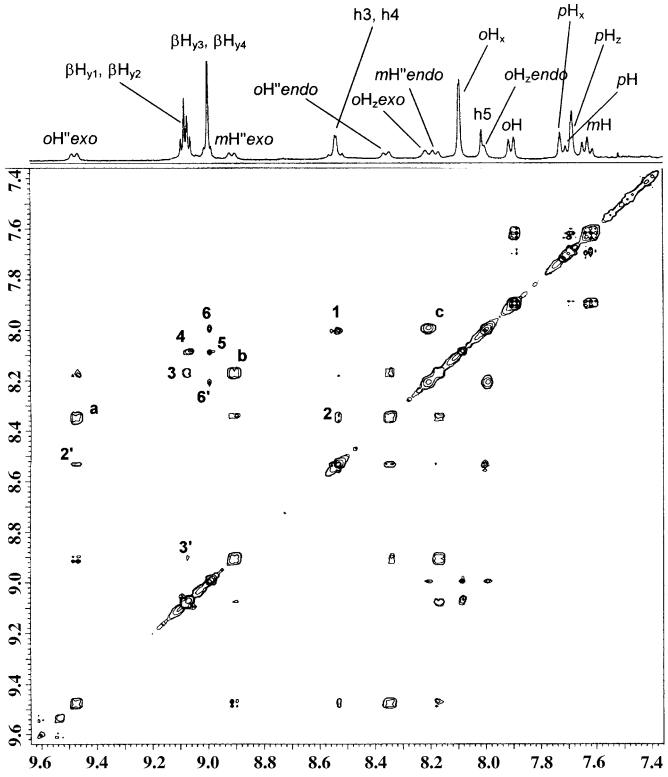

Figure 2. Downfield region of the 2D NOESY-EXSY spectrum ($CDCl_3$) of **1** at $-40\,^{\circ}C$; exchange peaks are marked with letters, while NOE peaks are numbered (2,2′; 3,3′; 6,6′ identify exchange NOE connections). See Scheme 1 for labeling and numbering scheme.

intensities, indicates that the symmetry of the bridging porphyrin is maintained in the adduct; compared to free **4′-*cis*DPyP** these resonances are spread over a wider range of chemical shifts ($\delta = 8.62$, 8.37, 7.50, and 7.32) due to the anisotropic shielding cones of the axial zinc porphyrin units.[15, 16] The resonances of the phenyl rings of **ZnP$_2$** in *meso* position 5 (*o*H″ and *m*H″) and those of the *ortho* protons of the phenyl ring in *meso* position 20 (*o*H$_x$) broaden on formation of **1**; each of these resonances splits into two signals of equal intensity on lowering the temperature, this effect being particularly significant for *o*H″ and *m*H″ (Figure 1). In agreement with the formation of a 1:1 cyclic adduct, these phenyl rings in **1** have one side oriented towards the inside (*endo*) and the other towards the outside (*exo*) of the macrocycle; thus, the *endo* protons are more shielded by the combined anisotropic cones of the three porphyrin units than the corresponding *exo* protons and therefore resonate further upfield. At room temperature the rotation around the C*meso*–C*ring* bond is relatively fast on the NMR timescale, and the corresponding signals are averaged. On lowering the temperature the rotation becomes slow on the NMR timescale, and *endo* and *exo* protons have resolved signals (below $-20\,^{\circ}C$ for *o*H″ and *m*H″; below $-40\,^{\circ}C$ for *o*H$_x$; Figure 1). Accordingly, in the 2D EXSY-NOESY spectrum of **1** at $-40\,^{\circ}C$ each pair of resonances of *endo* and *exo* aromatic protons is connected by an exchange cross-peak (Figure 2).

In addition, as the two oblique zinc porphyrin units in **1** induce large shifts in the resonances of the axial bridging **4′-*cis*DPyP**, resolution of the signal for the internal NH protons into three resonances can be expected if the rate of the tautomeric equilibrium that exchanges positions I and III with II and IV is sufficiently slow on the NMR timescale (Figure 3). Indeed, upon lowering the temperature the NH protons of **4′-*cis*DPyP** in **1** at first showed strong broadening and then split into three signals at $\delta = -3.67$, -3.89, and -4.05 with 1:2:1 relative integration. The central resonance with double intensity was assigned to the protons in the equivalent positions I and III, while the upfield resonance was attributed to the proton in position II, closest to the shielding cone of the two zinc porphyrin units (Figure 3). The reduced rate of tautomeric equilibrium also affects the resonances of the pyrrole protons of **4′-*cis*DPyP** (βH): at $-50\,^{\circ}C$ each splits into two equally intense signals, as expected. However, owing to the presence of several resonances in this region of the spectrum, only some of them do not overlap with other signals, and thus complete assignment was not possible.[17] This phenomenon has already been described by Imamura et al. for a trimer composed of two Os(OEP)(CO) units axially coordinated to **4′-*cis*DPyP** (OEP = 2,3,7,8,12,13,17,18-octaethylporphyrin).[18]

Absorption and luminescence spectroscopy: The NMR data obtained in $CDCl_3$ solution clearly indicated that **1** is formed from its components with a large association constant K_a. A quantitative determination of K_a was performed by means of

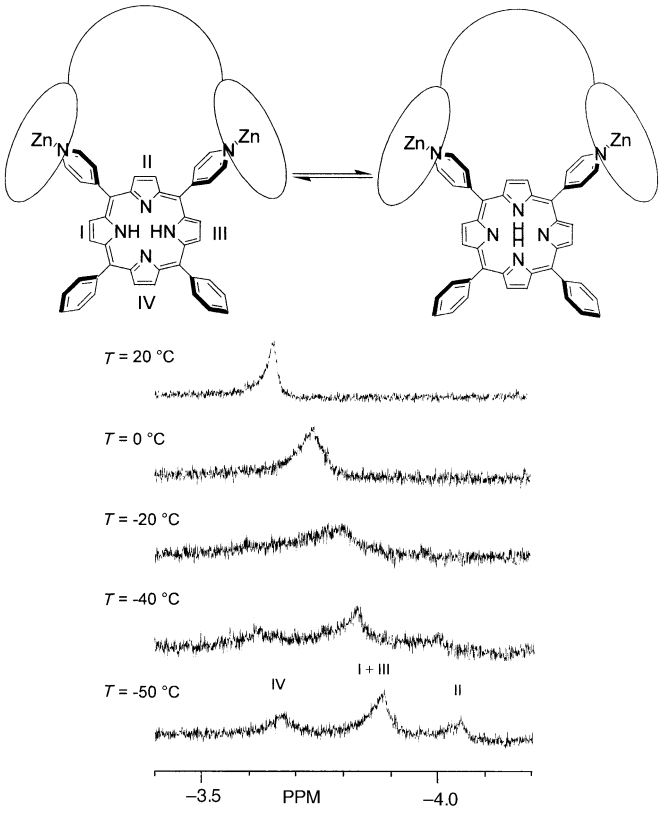

Figure 3. Schematic representation of NH tautomeric equilibrium of **4′-*cis*DPyP** in **1** and VT ^{1}H NMR spectra of NH resonance of **4′-*cis*DPyP** showing low-temperature resolution into three signals.

absorption and emission titration experiments in toluene.[19] The absorption spectrum of uncomplexed **4′-*cis*DPyP** displays an intense Soret band at 419 nm and four Q bands with maxima at 514, 547, 590, and 645 nm, in excellent agreement with other free-base dipyridyl porphyrins.[8b, 13] The spectrum of $\mathbf{ZnP_2}$ is the sum of the spectral properties of the individual constituents: an intense Soret band at 424 nm and Q bands at 551 and 591 nm due to the porphyrinic components, and a broad absorption around 300 nm due to the phenanthroline chromophore.[13] Thus, it can be safely assumed that the components of $\mathbf{ZnP_2}$ interact only weakly.

Addition of increasing amounts of **4′-*cis*DPyP** to a constant concentration of $\mathbf{ZnP_2}$ induces spectral changes in the resulting mixture that are not consistent with the simple superposition of the spectra of the two fragments.[13] In fact, it is well known that on axial coordination of pyridyl residues, the absorption bands of zinc porphyrins display a red shift of a few nanometers.[6c, 8b, 20] For a quantitative treatment of the absorption data it is convenient to define a derived spectral profile $\Delta A(\lambda)$ as the difference between the experimental absorbance detected for the mixture and the cumulative absorbances of the individual components at any given concentration.[8b] Figure 4 shows $\Delta A(\lambda)$ for a series of increasing **4′-*cis*DPyP** concentrations in 4.3×10^{-7} M toluene solutions of $\mathbf{ZnP_2}$. Equation (1) can be used to derive the association constant $K_a = 1/K_d$:

$$Obs = Obs_0 + \frac{\Delta Obs}{2S_0}\{K_d + X + S_0 - [(K_d + X + S_0)^2 - 4XS_0]^{1/2}\} \quad (1)$$

where *Obs* is an observable (e.g., absorbance or emission intensity), S_0 is the concentration of $\mathbf{ZnP_2}$ (constant), X is the concentration of **4′-*cis*DPyP** (variable), and ΔObs is the maximum variation of the observable under examination.[8b, 21] Fitting the data points at 433 nm (inset of Figure 4) reveals a 1:1 stoichiometry for **1** and gives an association constant of $8 \times 10^8\,\mathrm{M}^{-1}$.

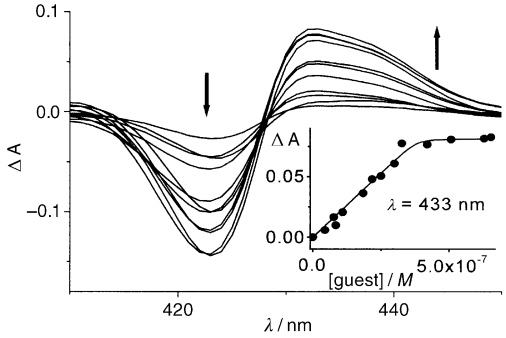

Figure 4. ΔA (see text for details) for a series of toluene solutions containing 4.3×10^{-7} M $\mathbf{ZnP_2}$ and increasing concentrations of **4′-*cis*DPyP** (from 4.4×10^{-8} to 6.5×10^{-6} M). In the inset the data points at 433 nm are fitted according to Equation (1).

The luminescence spectra of optically matched solutions of $\mathbf{ZnP_2}$ and **4′-*cis*DPyP** excited at 422 nm are shown in Figure 5, and the luminescence decays measured in a single-photon time-correlated apparatus (1 ns resolution) appear in the inset.

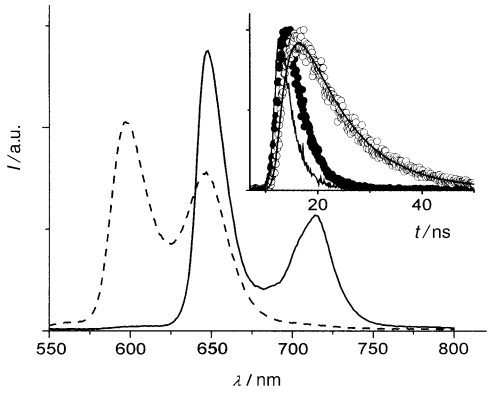

Figure 5. Luminescence spectra of optically matched toluene solutions ($A = 0.29$) of $\mathbf{ZnP_2}$ (dashed) and **4′-*cis*DPyP** (continuous line) on excitation at 422 nm. In the inset the luminescence decay of the solutions and fittings measured at 650 nm for **4′-*cis*DPyP** (○) and at 600 nm for $\mathbf{ZnP_2}$ (●) are shown together with the flash profile (——).

The luminescence properties of the two components of **1** at 298 and 77 K are summarized in Table 1. The luminescence of a $\mathbf{ZnP_2}$ solution is modified by addition of increasing concentrations of **4′-*cis*DPyP** in a way that is not consistent with the simple addition of the luminescence from the individual components. It is again convenient to define a derived spectral profile $\Delta I(\lambda)$ as the difference between the experimental luminescence intensity detected for the mixture and the luminescence intensity of **4′-*cis*DPyP** at a given concentration. The $\Delta I(\lambda)$ determined on excitation at 428 nm

Table 1. Photophysical properties of **ZnP_2** and ***4′-cis*DPyP** in toluene.

	State	298 K λ_{max} [nm]	τ [ns]	Φ_{fluo}[a]	77 K λ_{max} [nm]	τ [ns]	E [eV][b]
ZnP_2	$^1ZnP_2$	597, 648	2.0	0.065	602, 658	2.8	2.06
	$^3ZnP_2$				788		1.57
***4′-cis*DPyP**	^{1}4′-*cis*DPyP	648, 714	9.3	0.11	640, 710	14.8	1.94
	^{3}4′-*cis*DPyP				774		1.60

[a] Fluorescence quantum yields; see Experimental Section for details. [b] Determined from the emission maxima at 77 K.

(isosbestic point of the complexed and uncomplexed forms of **ZnP_2**) for addition of increasing concentrations of ***4′-cis*DPyP** to 4.3×10^{-7} M toluene solutions of **ZnP_2** are reported in Figure 6. The band at 600 nm, ascribable only to the **ZnP_2** component, decreases, and the band at 714 nm, typical of ***4′-cis*DPyP**, correspondingly increases. This effect, due to the

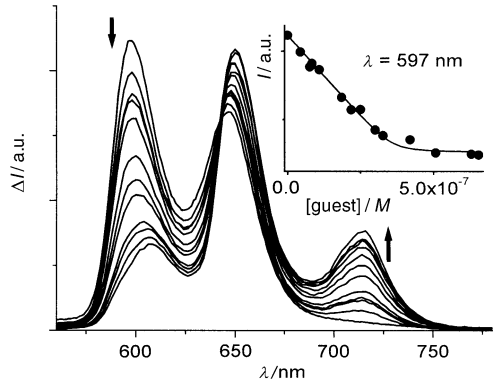

Figure 6. ΔI (see text for details) for a series of toluene solutions containing 4.3×10^{-7} M **ZnP_2** and increasing concentrations of ***4′-cis*DPyP** (from 0 to 6.5×10^{-6} M). In the inset the data points at 597 nm are fitted according to Equation (1).

quenching of the host fluorescence and the sensitization of the guest fluorescence, can be correlated with complex formation. Indeed, fitting the luminescence signal in the region of the exclusive **ZnP_2** emission according to Equation (1) yields an association constant of 4×10^8 M^{-1} for the 1:1 complex (inset of Figure 6). In view of the large errors (see Experimental Section) generally involved in this type of determination this value can be considered to be in reasonable agreement with the value of 8×10^8 M^{-1} derived from the absorption signals. The two results can be averaged to obtain $K_a = 6\times10^8$ M^{-1}.

X-ray structure: The X-ray diffraction analysis of crystals obtained from $CDCl_3$ confirms that in **1** the bis(pyridyl)porphyrin unit is axially coordinated to both the zinc centers of **ZnP_2** to form a multiporphyrin macrocyclic assembly. Figure 7 shows two space-filling views of **1**. The planes of the phenanthroline moiety and of ***4′-cis*DPyP**, which have a coplanar arrangement, are almost orthogonal to the porphyrin units of **ZnP_2**. The planes through the zinc porphyrin units of **ZnP_2** form dihedral angles of 80.7(2) and 84.6(2)° with the phenanthroline mean plane, and 88.7(1) and 88.9(1)° with the ***4′-cis*DPyP** mean plane. The former values, when compared with those found for the two crystallographically independent molecules of **ZnP_2** [46 and 81° (A); 68 and 73° (B)],[12]

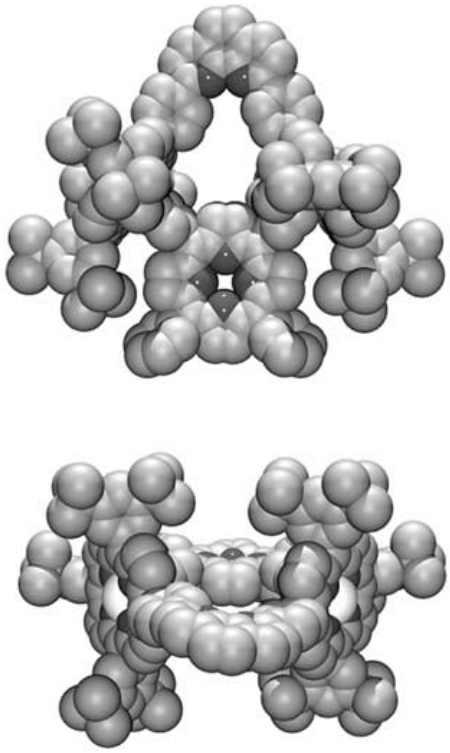

Figure 7. Two perspective views of the solid-state molecular structure of **1** in space-filling (CPK) representation.

indicate that coordination of ***4′-cis*DPyP** between the two zinc porphyrins is accompained by conformational changes of the host. Therefore, compound **1** has a C_{2h} symmetry, although some distortions are apparent from the crystal structure, such as the different arrangement of the arene groups at the *meso* positions of **ZnP_2** and the bowed conformation of the 2,9-diaryl-1,10-phenanthroline linker and the ***4′-cis*DPyP** moiety. The Zn···Zn distance in **1** (14.045(5) Å), which is slightly longer than the corresponding intermetallic distances measured in **ZnP_2** (13.79 and 13.44 Å),[12] evidences a slight widening of the zinc porphyrin bite. Thus, the **ZnP_2** fragment in **1** maintains its original oblique V-shaped arrangement, but complexation with ***4′-cis*DPyP** induces a more symmetrical arrangement of the two zinc porphyrin units, the mean planes of which now form a dihedral angle of 66.2(1)°.

The two Zn^{2+} cations exhibit very similar square-pyramidal coordination geometries, and the Zn–N bond lengths for the axial positions (2.106(11) – 2.134(11) Å) are slightly longer than those in the equatorial plane (2.024(11) – 2.118(12) Å). The Zn atoms are displaced by about 0.3 Å from the basal plane towards the apical pyridyl ligand. The phenyl rings (Ph) at positions 2 and 9 of the phenanthroline spacer (phen) are only slightly tilted with respect to the phen mean plane (dihedral angles of 20.2(7) and 24.3(6)°). This almost coplanar arrangement allows delocalization of π electrons over the Ph – phen – Ph system.

The crystal packing of **1** involves pairs of molecules arranged about a center of symmetry with two ***4′-cis*DPyP** units stacked on top of each other (Figure 8). Since each pyridylporphyrin assumes a conformation that is bent outward with respect to the inversion center, the shortest contact

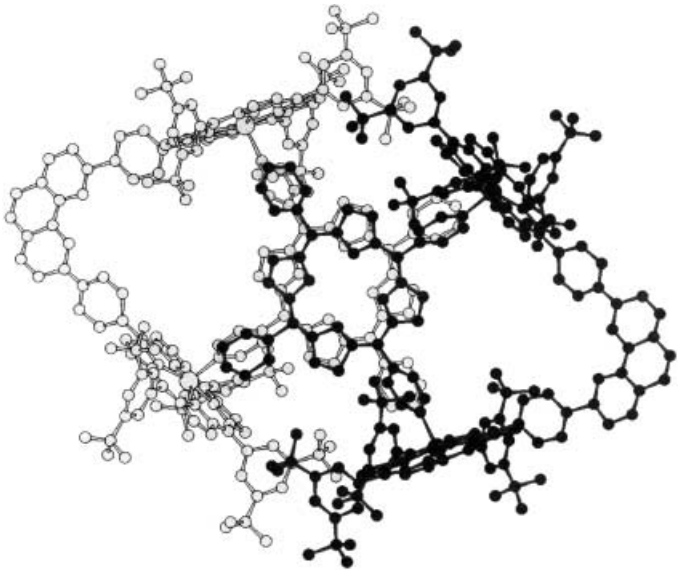

Figure 8. Schematic drawing of two molecules of **1** in the crystal arranged about a symmetry center, showing the stacking interaction between the ***4′-cis*DPyP** moieties.

is between the nitrogen atoms inside the porphyrin core, with a mean distance of 3.81 Å.

The fact that the solid-state structure is in good agreement with the ^{1}H NMR spectrum of **1** in $CDCl_3$ indicates that the same average architecture also exists in solution. Crystals of **1** dissolved in $CDCl_3$ gave the same ^{1}H NMR spectrum as described above.

Photoinduced processes: Photophysical studies were carried out on toluene solutions.[19] On formation of complex **1** the fluorescence of $\mathbf{ZnP_2}$ is quenched and the corresponding fluorescence of the ***4′-cis*DPyP** component is sensitized (Figure 6). This result can be interpreted on the basis of energy transfer from the lowest singlet excited state of the $\mathbf{ZnP_2}$ component to the lowest singlet excited state of the ***4′-cis*DPyP** component in **1**. The energies of these excited states are 2.06 eV for $\mathbf{ZnP_2}$ and 1.94 eV for ***4′-cis*DPyP** (Table 1), from which a ΔG^0 value of -0.12 eV is derived for the energy-transfer process. This process is therefore moderately exergonic and is expected to occur rapidly. Time-resolved experiments with 20 ps resolution indicate a lifetime of 50 ps for the decay of the luminescence of the $\mathbf{ZnP_2}$ component, measured at 610 nm; the same lifetime was measured for the rise of the luminescence of the ***4′-cis*DPyP** band at 715 nm, and thus the occurrence of the postulated intramolecular energy transfer in **1** is established. In Figure 9 the evolution of the luminescence with time at the above two wavelengths is shown with an exponential fitting corresponding to 50 ps at both wavelengths. In the inset of Figure 9, the time-resolved spectrum in the time window immediately after excitation (0–80 ps) is compared with the spectrum detected well after excitation (600–680 ps) and clearly indicates that the $\mathbf{ZnP_2}$ luminescence band (600 nm) present in the early stages disappears and is later replaced by the ***4′-cis*DPyP** luminescence band (715 nm).

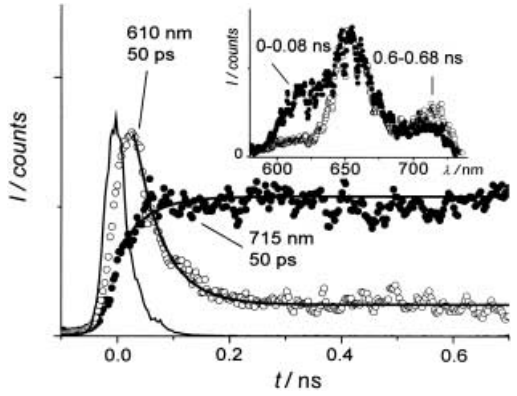

Figure 9. Luminescence time profiles and exponential fitting for a 1:1 toluene solution of $\mathbf{ZnP_2}$ and ***4′-cis*DPyP** at selected wavelengths. Time-resolved spectra collected in a time window of 80 ps at different time delays are displayed in the inset.

On the basis of a lifetimes of 50 ps (τ) for $\mathbf{ZnP_2}$ in **1** and 2 ns (τ_0) for uncomplexed $\mathbf{ZnP_2}$ (Table 1), a rate $k_{en} = 2 \times 10^{10}\ s^{-1}$ can be calculated for the energy-transfer process by using the equation $k_{en} = 1/\tau - 1/\tau_0$.

Energy transfer between singlet states can occur by two mechanisms: the Förster mechanism (dipole–dipole interaction) and the Dexter mechanism (electron exchange).[22, 23] For the former case the rate k_{en}^F can be accurately calculated by means of Equation (2)[22]

$$k_{en}^F = \frac{8.8 \times 10^{-25}\,\kappa^2 \Phi}{n^4 \tau d_{DA}^6} J^F \qquad (2)$$

where Φ and τ are the emission quantum yield (0.065) and lifetime (2 ns) of the donor $\mathbf{ZnP_2}$, respectively, d_{DA} is the donor–acceptor center-to-center distance (10.1 Å), n the refractive index of toluene, and J^F the overlap integral. The calculated value of J^F is $3.43 \times 10^{-14}\ cm^3\,M^{-1}$,[22b] and Equation (3) can be derived.

$$k_F^{en} = 3 \times 10^{11}\ s^{-1}\,\kappa^2 \qquad (3)$$

where κ^2, the orientation factor, takes into account the relative orientation of the transition dipole moments of the donor and the acceptor. For a pair of reacting partners which freely diffuse in solution, the value is statistical (0.6667), since they approach one another randomly. The statistical value for κ^2 is clearly not applicable when the two partners are locked in rigid positions with respect to each other. From Equation (2) and the experimental rate $k_{en} = 2 \times 10^{10}\ s^{-1}$, a κ^2 value of 0.066 can be calculated for **1**, under the assumption that quenching occurs exclusively by a Förster mechanism. This assumption is justified by the good overlap of the emission of the donor and the absorption of the acceptor [Figure 5 and Figure S5 (Supporting Information)]. If the Dexter mechanism contributes to the process of energy transfer, κ^2 would have even lower values. The calculated $\kappa^2 = 0.066$, which is considerably lower than the statistical value, is in agreement with previous studies and shows that we are dealing with a well-defined, stable assembly in which the energy transfer partners are locked in rigid positions that are unfavorable for interactions of transition dipole moments.[8b, 24]

This consideration was supported by measurements in glassy toluene solutions at 77 K, in which a lifetime of 370 ps was measured for the donor showing a tenfold decrease of the energy transfer rate (from 2×10^{10} s^{-1} at 298 K to 2.3×10^{9} s^{-1} at 77 K; Table 1). This decrease is remarkable for exergonic energy-transfer reactions, which are usually temperature-independent.[25] Likely, the rigidification of the solvent prevents internal molecular motions that can facilitate a favorable orientation of the transition dipoles involved in Förster energy transfer. Note that although the X-ray structure shows an almost perpendicular orientation of the chromophores, this orientation cannot be extrapolated to solution conditions.

It is interesting to compare the present results to those obtained in a similar adduct based on oblique dizinc bis-porphyrinic hosts encapsulating a free base. In our case the light energy collected by $\mathbf{ZnP_2}$ is conveyed with 98% efficiency to the free-base **4′-*cis*DPyP** (antenna effect), which plays the role of an energy sink. A similar behavior is observed in most free-base/zinc porphyrin dyads in which the excited singlet state of the zinc component lies above that of the free-base fragment.[7b, 26] The opposite behavior found in the macrocycles based on the dizinc bis-porphyrin host synthesized by Johnston et al.,[7b] that is, photoinduced energy transfer from the free-base guest to the host,[8b] is an exception and must be ascribed to the presence of quinazoline groups at the periphery of the zincated host, which lowers its excited-state energy (1.86 vs 2.06 eV for $\mathbf{ZnP_2}$).[8a]

Conclusion

The quantitative formation in solution of a 1:1 tris-porphyrin macrocyclic assembly with a 36-membered ring between the oblique dizinc(II) bis-porphyrin system $\mathbf{ZnP_2}$ and **4′-*cis*DPyP** was shown to occur through the formation of two axial 4′-N(pyridyl)–Zn interactions. An association constant of about 6×10^{8} M^{-1} was measured by both UV/Vis absorption and emission titrations. The assembly was fully characterized in solution by NMR spectroscopy. Furthermore, the complex was characterized by X-ray crystallography. Solid-state data confirmed the almost perfect size match between **4′-*cis*DPyP** and $\mathbf{ZnP_2}$, reflected in the very small conformational changes induced in the dizinc bis-porphyrin moiety by axial coordination of **4′-*cis*DPyP**. To our knowledge this is the first time that the solid-state structure of a macrocyclic porphyrin assembly of this kind has been determined.

The photophysical data in toluene indicate that **1** has useful photophysical features as a donor–acceptor multiporphyrin conjugate: the free-base porphyrin guest behaves as an energy sink that displays almost quantitative collection of the light energy absorbed by the two zinc porphyrin units, the main chromophores of the system, on irradiation.

The present synthetic strategy represents a new and convenient noncovalent approach to the construction of large rings incorporating various electrophores and chromophores, such as porphyrins. Simple mixing at room temperature of two classical porphyrinic fragments, already described in the literature many years ago,[12, 27, 28] leads to the quantitative assembly of a highly stable macrocycle. Formation of multi-macrocyclic species can be anticipated if **4′-*cis*DPyP** is replaced by a species with more than two appended pyridyl ligands. In particular, 5,10,15,20-tetra(4′-pyridyl)porphyrin and related fragments bearing peripheral ligands properly disposed to interact with the zinc atoms of $\mathbf{ZnP_2}$ are particularly promising (e.g. **II**). In addition, we will investigate the capability of the bis-porphyrin difunctional receptor $\mathbf{ZnP_2}$ to discriminate between dipyridylporphyrins of different geometries, for example, **4′-*cis*DPyP** versus **4′-*trans*DPyP**.

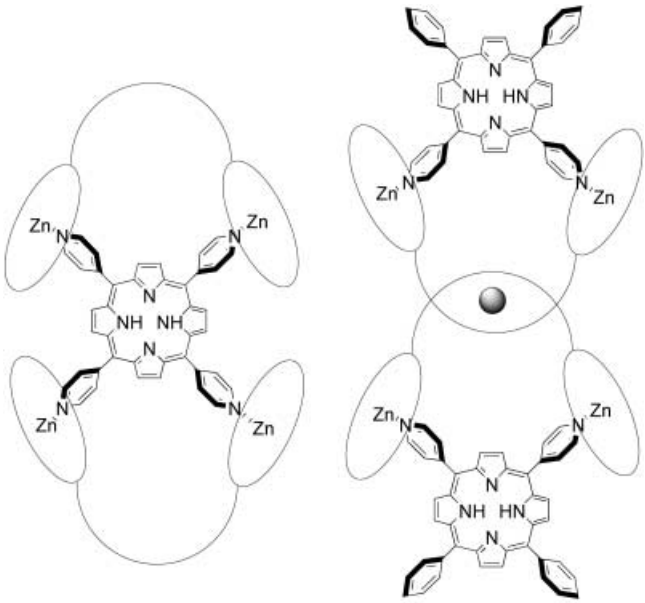

Interestingly, the macrocyclic species is functionalized with a chelating unit (phen) which can be exploited in subsequent reactions to incorporate transition metals, such as tetrahedral Cu^{I},[10] and trigger various coordination reactions, possibly leading to higher order multicomponent species. Of particular interest is the potential of the cyclic compound **1** as a precursor building block to threaded rings, such as catenanes (e.g., **III**). These higher order architectures might display an enhanced antenna effect. Inclusion of a Cu^{I}–phen unit in the array introduces metal-to-ligand charge transter (MLCT) excited states of low energy localized on the metal complex, which could, in principle, compete for energy collection with the free-base porphyrin.[10c] Nonetheless, the reaction rate constant we previously determined for the transfer of energy from the zinc porphyrin donor to the Cu^{I} complex acceptor in an essentially identical structure is 5×10^{9} s^{-1},[10c] which can be compared with the rate determined here for energy transfer from the zinc porphyrin to the free-base porphyrin acceptor of 2×10^{10} s^{-1}. This could, at most, reduce the efficiency of energy transfer from the zinc porphyrin to the free base-porphyrin to a still remarkably high 80%.

Experimental Section

General methods: **4′-*cis*DPyP** was prepared and purified as described before.[15] **Zn_2P** was synthesized as previously reported.[27]

^{1}H NMR spectra were recorded at 400 MHz on a JEOL Eclipse 400 FT instrument. All spectra were recorded at room temperature in $CDCl_3$ (Aldrich), unless otherwise stated. Proton peak positions were referenced to the peak of residual nondeuterated chloroform at $\delta = 7.26$. Assignments were made with the aid of 2D correlation spectroscopy (H,H-COSY) and 2D exchange spectroscopy (NOESY-EXSY) experiments, as detailed in the text; a mixing time of 500 ms was used for NOESY-EXSY experiments.

Titration experiments for the determination of the association constant were performed with a constant concentration of host **ZnP_2** and variable concentrations of guest **4′-*cis*DPyP**. Precise aliquots of **4′-*cis*DPyP** solutions in dichloromethane were vacuum dried and then dissolved in toluene or solutions of **ZnP_2** in toluene. The absorption and emission spectra of reference solutions containing only **4′-*cis*DPyP** or **ZnP_2** at each concentration used were determined together with those of **4′-*cis*DPyP**/**ZnP_2** mixtures. The estimated error in the determination of the association constants is on the order of $\pm 30\%$.

Absorption spectra were recorded with a Perkin–Elmer Lambda 9 spectrophotometer, and emission spectra, uncorrected if not otherwise noted, were detected with a Spex Fluorolog II spectrofluorimeter equipped with a Hamamatsu R928 photomultiplier. In the titration experiments, excitation was performed at the isosbestic point for the absorptions of **ZnP_2** in the uncomplexed and complexed forms. Relative luminescence intensities were evaluated from the area (on an energy scale) of the luminescence spectra, corrected for the photomultiplier response. Luminescence quantum yields ϕ for the components were obtained with reference to a Zn^{II} 5,10,15,20-tetra(4′-*tert*-butylphenyl)porphyrin standard in toluene with $\phi = 0.08$.[29] Luminescence lifetimes in the range 20–2000 ps were determined by an apparatus based on a Nd/YAG laser (Continuum PY62-10) with a 35 ps pulse at 10 Hz, 532 nm excitation, 1 mJ per pulse, and a Streak Camera.[30] Lifetimes longer than 2 ns were detected by an IBH time-correlated single-photon counting apparatus with excitation at 337 nm. Fitting of the luminescence decays was performed by standard iterative nonlinear programs taking into consideration the instrumental response. Air-equilibrated samples in 10 mm quartz cuvettes were used and, for luminescence experiments at 77 K, quartz capillary tubes with the samples were immersed in liquid nitrogen contained in a home-made quartz Dewar. Estimated errors are 10% for lifetimes and 20% for quantum yields.

The integral overlap and the rates of energy transfer by Dexter or Förster mechanisms were calculated with Matlab 5.2 (MatWorks).[31]

UV/Vis spectra in toluene (λ_{max} [nm] ε [$cm^{-1}M^{-1}$]): **4′-*cis*DPyP**: 419 (381000), 514 (18600), 547 (6800), 590 (5500), 645 (2900); **ZnP_2**: 424 (896500), 551 (43250), 591 (12700).

ZnP_2(4′-*cis*DPyP) (**1**): The multiporphyrin macrocyclic adduct **1** was obtained by addition of one equivalent of **4′-*cis*DPyP** to a solution of **ZnP_2** in $CDCl_3$ (ca. 4×10^{-3} M); the reaction was monitored by ^{1}H NMR spectroscopy and the ratio of the reactants adjusted accordingly. Analytically pure purple crystals of **1** were obtained by addition of *n*-hexane to the solution. Yield of isolated product: ca. 80%. UV/Vis spectrum in toluene (λ_{max} [nm] ε [$cm^{-1}M^{-1}$]): 425 (854800), 514 (22800), 556 (31900), 603 (17300). ^{1}H NMR at ambient temperature: $\delta = 9.08$ (βH_y, 4H, d), 9.08 (βH_y, 4H, d), 8.97 ($\beta H_y + oH$, 12H), 8.62 (βH, 2H, s), 8.54 (4H, m, H3,4phen; H7,8phen), 8.37 (2H, br d, βH), 8.11 (oH_z, 4H, m), 8.09 (oH_x, 8H, m), 7.99 (2H, s, H5,6phen), 7.90 (oH, 4H m), 7.77 (pH_z, m, 4H), 7.68 (2H, m, pH), 7.61 (4H, m, mH), 7.50 (2H, br d, βH), 7.32 (2H, br s, βH), 6.26 (4H, br s, H3,5), 2.98 (4H, v b s, H2,6), 1.55 (36H, s, tBu_z), 1.54 (18H, s, tBu_x), −3.65 (2H, br s, NH).

Crystal data for 1: $C_{190}H_{182}N_{16}Zn_2 \cdot 5.5\,CHCl_3$, $M = 3478.80$, triclinic, space group $P\bar{1}$, $a = 16.396(4)$, $b = 26.852(5)$, $c = 26.946(5)$ Å, $\alpha = 68.49(2)$, $\beta = 85.94(2)$, $\gamma = 75.03(2)^\circ$, $V = 10659(6)$ Å^3, $Z = 2$, $\rho_{calcd} = 1.084$ g cm^{-3}, $\mu = 2.552$ mm^{-1}, $F(000) = 3630$, 14119 unique reflections, $R1(I > 2\sigma(I)) = 0.1304$, $wR2 = 0.2929$, GOF = 1.227 for 6401 observed reflections ($I > 2\sigma(I)$) and 997 parameters.

The intensity data were collected at the X-ray diffraction beamline of Elettra Synchrotron (Trieste, Italy), on a 30 cm MAR2000 image plate with a monochromatic wavelength ($\lambda = 1.0000$ Å) by the rotating-crystal method to $2\theta_{max} = 53.2^\circ$ at 100 K. Data reduction and cell refinement were carried out by using the programs Mosflm and Scala.[32] The structure was solved by direct methods and successive Fourier analyses (SHELXS-97) and refined by full-matrix least-squares procedures on F^2 (SHELXL-97).[33] The carbon atoms were isotropically treated with hydrogen atoms at geometrically calculated positions. All the calculations were performed by using the WinGX System, Ver 1.64.03.[34]

A difference Fourier map revealed the presence of 2.5 molecules of $CHCl_3$ per asymmetric unit. Additional solvent molecules included in the formula were used for density calculation, by taking into account the analysis of the accessible voids in the unit cell obtained with the Platon package.[34] CCDC-198481 contains the supplementary crystallographic data for this paper. These data can be obtained free of charge via www.ccdc.cam.ac.uk/conts/retrieving.html (or from the Cambridge Crystallographic Data Centre, 12 Union Road, Cambridge CB21EZ, UK; fax: (+44) 1223-336-033; or deposit@ccdc.cam.uk).

Acknowledgement

The contributions of grant Agenzia2000 CNRC00B91D 004 and grant Agenzia2000 CNRC000951 are gratefully acknowledged. COST Project D11/0004/98 is also acknowledged. The CNR staff at ELETTRA (Trieste) are acknowledged for help in the use of the facility supported by CNR and by Elettra Scientific Division.

[1] a) J. Deisenhofer, H. Michel, *Angew. Chem.* **1989**, *101*, 872–892; *Angew. Chem. Int. Ed. Engl.* **1989**, *28*, 829–847; b) R. Huber, *Angew. Chem.* **1989**, *101*, 849–871; *Angew. Chem. Int. Ed. Engl.* **1989**, *28*, 848–869.

[2] a) T. Pullerits, V. Sundström, *Acc. Chem. Res.* **1996**, *29*, 381–389; b) G. McDermott, S. M. Prince, A. A. Freer, A. M. Hawthornwaite-Lawless, M. Z. Paziz, R. J. Codgell, N. W. Isaacs, *Nature* **1995**, *374*, 517–521; c) R. J. Codgell, N. W. Isaacs, A. A. Freer, J. Arrelano, T. D. Howard, M. Z. Paziz, A. M. Hawthornwaite-Lawless, S. M. Prince, *Prog. Biophys. Mol. Biol.* **1997**, *68*, 1–27.

[3] G. T. Babcock, M. Wikström, *Nature* **1992**, *356*, 301–309.

[4] J.-C. Chambron, V. Heitz, J.-P. Sauvage in *The Porphyrin Handbook*, *Vol. 6* (Eds.: K. M. Kadish, K. M. Smith, R. Guilard), Academic Press, San Diego, CA, **2000**, Chapter 40.

[5] a) C. A. Hunter, C. M. R. Low, M. J. Packer, S. E. Spey, J. G. Vinter, M. O. Vysotsky, C. Zonta, *Angew. Chem.* **2001**, *113*, 2750–2754; *Angew. Chem. Int. Ed.* **2001**, *40*, 2678–2682; b) E. Stulz, Y.-F. Ng, S. M. Scott, J. K. M. Sanders, *Chem. Commun.* **2002**, 524–525; c) A. Tsuda, T. Nakamura, S. Sakamoto, K. Yamaguchi, A. Osuka, *Angew. Chem.* **2002**, *114*, 2941–2945; *Angew. Chem. Int. Ed.* **2002**, *41*, 2817–2821.

[6] a) H. Imahori, E. Yoshizawa, K. Yamada, K. Hagiwara, T. Okada, Y. Sakata, *J. Chem. Soc. Chem. Commun.* **1995**, 1133–1134; b) K. Yamada, H. Imahori, E. Yoshizawa, D. Goztola, M. R. Wasielewski, Y. Sakata, *Chem. Lett.* **1999**, 235–236; c) L. Flamigni, M. R. Johnston, L. Giribabu, *Chem. Eur. J.* **2002**, *8*, 3938–3947; d) L. Flamigni, M. R. Johnston, *New J. Chem.* **2001**, *25*, 1368–1370.

[7] a) R. A. Haycock, A. Yartsev, U. Michelsen, V. Sundström, C. A. Hunter, *Angew. Chem.* **2000**, *112*, 3762–3765; *Angew. Chem. Int. Ed.* **2000**, *39*, 3616–3619; b) M. R. Johnston, M. J. Gunter, R. N. Warrener, *Chem. Commun.* **1998**, 2739–2740.

[8] a) L. Flamigni, G. Marconi, M. R. Johnston, *Phys. Chem. Chem. Phys.* **2001**, *3*, 4488–4494; b) L. Flamigni, A. M. Talarico, F. Barigelletti, M. R. Johnston, *Photochem. Photobiol. Sci.* **2002**, *1*, 190–197.

[9] a) M. J. Crossley, L. G. Mackay, C. A. Try, *J. Chem. Soc. Chem. Commun.* **1995**, 1925–1927; b) D. Monti, L. La Monica, A. Scipioni, G. Mancini, *New J. Chem.* **2001**, *25*, 780–782; c) R. Paolesse, D. Monti, E. Venanzi, A. Froiio, S. Nardis, C. Di Natale, C. E. Martinelli, A. D'Amico, *Chem. Eur. J.* **2002**, *8*, 2476–2483; d) X. Huang, B. Borhan, B. H. Rickman, K. Nakanishi, N. Berova, *Chem. Eur. J.* **2000**, *6*, 216–224; e) M. Takeuchi, T. Imada, S. Shinkai, *J. Am. Chem. Soc.* **1996**, *118*, 10658–10659; f) J. N. H. Reek, A. P. H. J. Schenning, A. W. Bosman, E. W. Meijer, M. J. Crossley, *Chem. Commun.* **1998**, 11–12; g) M. R. Johnston, M. J. Latter, R. N. Warrener, *Aust. J. Chem.* **2001**, *54*, 633–

636; h) G. Proni, G. Pescitelli, X. Huang, N. Q. Quraishi, K. Nakanishi, N. Berova, *Chem. Commun.* **2002**, 1590–1591.
[10] a) N. Solladié, J.-C. Chambron, J.-P. Sauvage, *J. Am. Chem. Soc.* **1999**, *121*, 3684–3692; b) M. Andersson, M. Linke, J.-C. Chambron, J. Davidsson, V. Heitz, J.-P. Sauvage, L. Hammarström, *J. Am. Chem. Soc.* **2000**, *122*, 3526–3527; c) M. Linke, J.-C. Chambron, V. Heitz, J.-P. Sauvage, S. Encinas, F. Barigelletti, L. Flamigni, *J. Am. Chem. Soc.* **2000**, *122*, 11834–11844; d) M. Linke, J.-C. Chambron, N. Fujita, V. Heitz, J.-P. Sauvage, *New J. Chem.* **2001**, *25*, 790–796; e) M. Andersson, M. Linke, J.-C. Chambron, J. Davidsson, V. Heitz, L. Hammarström, J.-P. Sauvage, *J. Am. Chem. Soc.* **2002**, *124*, 4347–4362.
[11] a) S. Chardon-Noblat, J.-P. Sauvage, P. Mathis, *Angew. Chem.* **1989**, *101*, 631–632; *Angew. Chem. Int. Ed. Engl.* **1989**, *28*, 593–595; b) A. M. Brun, A. Harriman, V. Heitz, J.-P. Sauvage, *J. Am. Chem. Soc.* **1991**, *113*, 8657–8663; c) A. M. Brun, S. J. Atherton, A. Harriman, V. Heitz, J.-P. Sauvage, *J. Am. Chem. Soc.* **1992**, *114*, 4632–4639; d) A. Harriman, V. Heitz, J.-P. Sauvage, *J. Phys. Chem.* **1993**, *97*, 5940–5946; e) J.-C. Chambron, A. Harriman, V. Heitz, J.-P. Sauvage, *J. Am. Chem. Soc.* **1993**, *115*, 6109–6114; f) A. Harriman, V. Heitz, M. Ebersole, H. van Willigen, *J. Phys. Chem.* **1994**, *98*, 4982–4989.
[12] C. Pascard, J. Guilhem, S. Chardon-Noblat, J.-P. Sauvage, *New J. Chem.* **1993**, 331–335.
[13] See Supporting Information.
[14] E. Iengo, S. Geremia, E. Zangrando, R. Minatel, E. Alessio, *J. Am. Chem. Soc.* **2002**, *124*, 1003–1013.
[15] E. Alessio, M. Macchi, S. L. Heat, L. G. Marzilli, *Inorg. Chem.* **1997**, *36*, 5614–5623.
[16] Assignments were made on the basis of the multiplicity of the signals and of the distance of the β-protons from the shielding zinc porphyrin units.
[17] The broadening of the βH resonances upon lowering the temperature to below 0 °C is so pronounced that they become almost undetectable in a 5 °C interval of temperature around −40 °C (see also the H,H-COSY spectrum of **1** in the Supporting Information).
[18] N. Kariya, T. Imamura, Y. Sasaki, *Inorg. Chem.* **1997**, *36*, 833–839.
[19] This solvent provides better photochemical and thermal stability of the dissolved porphyrin adduct in comparison with other typical organic solvents (e.g., dichloromethane). In addition, the high quality of toluene matrices at 77 K makes spectroscopic and photophysical determinations under these conditions convenient.
[20] See, for example, a) N. Armaroli, F. Diederich, L. Echegoyen, T. Habicher, L. Flamigni, G. Marconi, J. F. Nierengarten, *New J. Chem.* **1999**, *23*, 77–83; b) F. Felluga, P. Tecilla, L. Hillier, C. A. Hunter, G. P. Licini Scrimin, *Chem. Commun.* **2000**, 1087–1088; c) H. Shinmori, T. Kajiwara, A. Osuka, *Tetrahedron Lett.* **2001**, *42*, 3617–3620; d) J. Brettar, J.-P. Gisselbrecht, M. Gross, N. Solladié, *Chem. Commun.* **2001**, 733–734.
[21] a) C. S. Wilcox in *Frontiers in Supramolecular Organic Chemistry and Photochemistry* (Eds.: H. J. Schneider, H. Dürr), VCH, Weinheim, **1991**, pp. 122–143; b) S. Encinas, K. L. Bushell, S. M. Couchman, J. C. Jeffery, M. D. Ward, L. Flamigni, F. Barigelletti, *J. Chem. Soc. Dalton Trans.* **2000**, 1783–1792.
[22] a) T. Förster, *Discuss. Faraday Soc.* **1959**, *27*, 7–17; b) J^F is the Förster overlap integral calculated from Equation (3).[22a]

$$J^F = \frac{\int F(v)\,\varepsilon(v)/v^4 \mathrm{d}v}{\int F(v)\mathrm{d}v} \quad (3)$$

This represents the overlap integral between the luminescence spectrum of the donor **ZnP$_2$** $F(\bar{v})$ [cm^{-1}] and the absorption spectrum $\varepsilon(\bar{v})$ [cm^{-1}] of the acceptor ***4′-cis*DPyP**. From the experimental emission and absorption spectra, an overlap integral J^F of 3.4355×10^{-14} cm^3 M^{-1} was calculated.
[23] D. L. Dexter, *J. Chem. Phys.* **1953**, *21*, 836–850.
[24] L. Giribabu, A. A. Kumar, V. Neeraja, B. G. Maiya, *Angew. Chem.* **2001**, *113*, 3733–3736; *Angew. Chem. Int. Ed.* **2001**, *40*, 3621–3624.
[25] L. Hammarström, F. Barigelletti, L. Flamigni, N. Armaroli, A. Sour, J.-P. Collin, J.-P. Sauvage, *J. Am. Chem. Soc.* **1996**, *118*, 11972–11973.
[26] a) F. Odobel, S. Suresh, E. Blart, Y. Nicolas, J.-P. Quinterd, P. Janvier, J.-Y. Le Questel, B. Illien, D. Rondeau, P. Richomme, T. Häupl, S. Wallin, L. Hammarström, *Chem. Eur. J.* **2002**, *8*, 3027–3046; b) J.-S. Hsiao, B. P. Krueger, R. W. Wagner, T. E. Johnson, J. K. Delaney, D. C. Mauzerall, G. R. Fleming, J. S. Lindsey, D. F. Bocian, R. J. Donohoe, *J. Am. Chem. Soc.* **1996**, *118*, 11181–11193.
[27] S. Chardon-Noblat, J.-P. Sauvage, *Tetrahedron* **1991**, *47*, 5123–5132.
[28] E. B. Fleischer, A. M. Shacter, *Inorg. Chem.* **1991**, *30*, 3763–3769.
[29] I. M. Dixon, J.-P. Collin, J.-P. Sauvage, L. Flamigni, *Inorg. Chem.* **2001**, *40*, 5507–5517.
[30] L. Flamigni, *J. Phys. Chem.* **1993**, *97*, 9566–9572.
[31] Matlab 5.2, The MathWorks Inc., Natik, MA 01760 (USA).
[32] Collaborative Computational Project, Number 4, *Acta Crystallogr. Sect. D* **1994**, *50*, 760.
[33] G. M. Sheldrick, SHELX-97, Programs for Crystal Structure Analysis (Release 97-2), University of Göttingen, Germany, **1998**.
[34] WinGX—A Windows Program for Crystal Structure Analysis, L. J. Farrugia, *J. Appl. Crystallogr.* **1999**, *32*, 837–838.
[35] A. L.Spek, *Acta Crystallogr. Sect. A* **1990**, *46*, C34.

Received: January 31, 2003
Revised: May 12, 2003 [F4795]

